Long-period Ground Motion Simulation for NTF Fault Scenario in Tabriz City

Mohammad Reza Ghayamghamian
International institute of earthquake engineering and seismology, Tehran, Iran

Afrooz Rajool
Islamic Azad University, Tehran, Iran

SUMMARY:
Tabriz, one of the metropolises of Iran, is a megacity situated at the northwest of the Iran with more than 1.5 million inhabitants. North Tabriz Fault (NTF) is a major seismogenic fault in NW of Iran that crossed north of Tabriz city and directly threaten metropolitan area of Tabriz. The NTF would have been the source of several major historical earthquakes in the past. Therefore, it is an important task to identify the characteristics of long-period strong ground motions for seismic hazard mitigation plan and design of long structures. The kinematic model with non-uniform slip distribution on the fault plane is employed to simulate velocity waveforms at the sites. To this end, the source parameters for the worst rupture scenario of NTF are defined. Then, the long-period velocity motions for this rupture scenario are simulated at 300 points in a grid of 1 km × 1 km covering whole Tabriz region. The simulated motions clearly show near-fault directivity pulse with different peaks and periods depending on the site location to the fault. The peak velocity (PGV) is found to be in the range of 100 to 255 cm/sec. Furthermore, the response spectra for simulated motions are also calculated, which their peak values vary in the range of 200-330 cm/sec for velocity. Finally, the estimated peak ground velocities as well as their peak spectral values at the sites are used to develop velocity microzonation maps for Tabriz City.

Keywords: Near-fault directivity pulse, Ground motion simulation, Kinematic model, Asperity, PGV microzonation maps, Tabriz City.

1. INTRODUCTION

Tabriz is the fourth largest city and one of the historical capitals of Iran located in northwest of Iran in East Azerbaijan province between Eynali and Sahand mountains in a fertile area and the estimated population of the city is around 1,400,000. Tabriz is also a major Iranian heavy industrial and manufacturing center surrounded by several active faults which caused many destructive earthquakes in history of Iran and faced disastrous damages. To date, more than 12 historical earthquakes have been occurred in the Tabriz region. For example in earthquake 1779 with magnitude M_S=7.7, more than 50000 people died. Thus, the disaster mitigation and management are of great importance in Tabriz.

Northwest of Iran is a region of intense deformation and seismicity situated between two thrust belts of the Caucasus to the north and the Zagros Mountains to the south. Earthquake focal mechanisms suggest that the convergence between Arabia and Eurasia has been accommodated mainly through WNW-trending right-lateral strike-slip faults in this region (Fig. 1.1). The North Tabriz Fault (NTF) is one of the most important active faults that directly menacing this metropolitan and would have been the source of several major historical earthquakes in the past (Berberian 1983 and Ambrasys 1982) that has a clear surface expression. It has an average strike of NW-SE over a length of about

150 km and appears to be generally close to vertical in dip. Hessami *et al.* (2003) suggested that the slip rate along the NTF is about 3.1-6.4 mm/yr and they estimated the mean recurrence interval of NTF is in the range of 821±176 years. Therefore, the hazard mitigation studies for decreasing the damage severity from a most probable earthquake in future are inevitable.

Most of strong motion estimations in earthquake hazard analysis are still inclined to the probabilistic seismic hazard analysis (PSHA) method. In this method, attenuation relations have been used extensively to predict simple parameters characterizing ground motion intensity, such as peak ground acceleration (PGA) or spectral acceleration (SA), as a function of earthquake size and distance. Conventional attenuation relations predict ground motion parameters using simplified model in which the effects of earthquake source are presented by earthquake magnitude; the effects of wave propagation from the earthquake source to site are specified by a distance; and the effects of the site are specified by a simple site category. These relations have a large degree of uncertainty in the estimation of strong ground parameter, especially in the near-fault area (Ghayamghamian, 2007a). The damage distribution of the large earthquakes such as the Hyogo-ken Nanbu (1995, Japan), Kacaeli (1999, Turkey), Chi-Chi (1999, Taiwan), and Bam (2003, Iran) earthquakes revealed that the ground motions in near-fault area have two special characteristics, namely rupture directivity and fling effects, which need to be carefully treated in the seismic hazard evaluation.

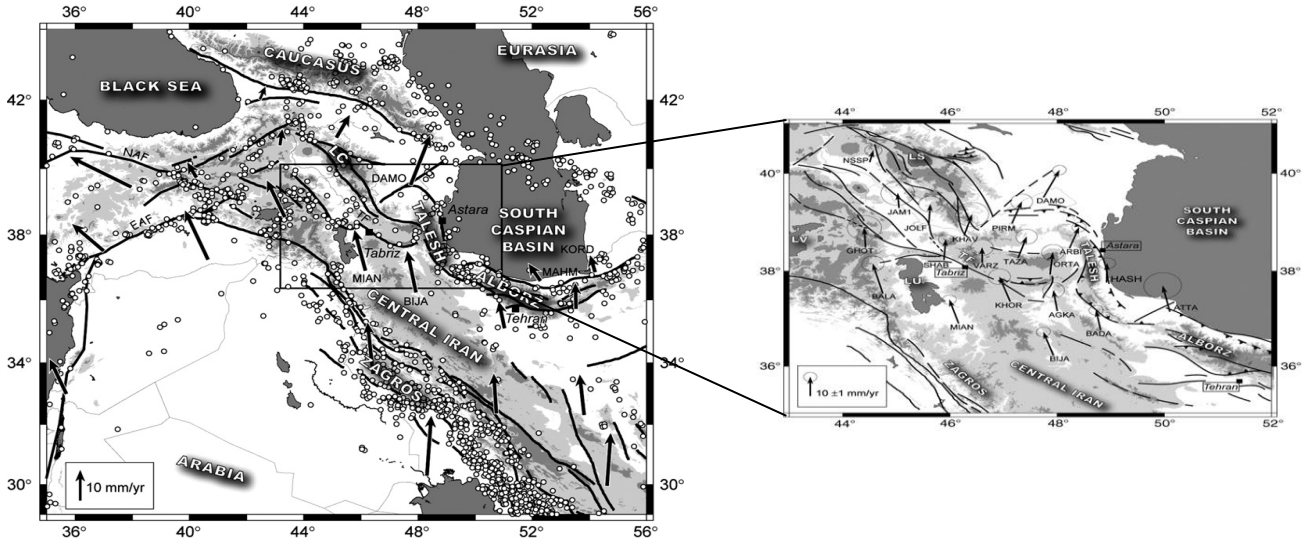

Figure 1.1. Map of the central part of the Arabia–Eurasia collision zone (Massone et al., 2006).

In principle, when an earthquake fault ruptures and propagates towards a site at a speed close to the shear wave velocity, the generated waves will arrive at the site at approximately the same time, generating a "distinct" velocity pulse in the ground motion time history in the strike-normal direction (Singh 1985, Somerville et al. 1997). This intense velocity pulse usually occurs at the beginning of a record. This is referred to as the forward directivity effect, which has been known for more than a decade to have the potential to cause severe damage to the structures (Bertero et al. 1978, Singh 1985, Hall et al. 1995, Hall 1998, Wald and Heaton 1998, Iwan et al. 2000, Aagaard et al. 2000 and 2001, Alavi and Krawinkler 2001 and 2004, MacRae et al. 2001). The analyses of elastic and inelastic multiple degree of freedomsystem indicates that the amplitude and period of the pulse in the velocity time history are key parameters which control the performance of structures (Krawinkler and alavi 2000). Furthermore, many researchers have shown that a ground motion with a distinct velocity pulse tends to cause heightened elastic response only in a

narrow period range of structures, namely those with a natural period close to the pulse period(e.g., Alavi and Krawinkler 2001, Mavroeidis and Papageorgiou 2003, Somerville 2003, Baker and Cornell 2005, Fu 2005, Tothong and Cornell 2006a, Tothong and Cornell 2007). Then, the question will be how to estimate the ground motion hazard for a site that may experience such a forward directivity effect.

In this paper, long-period ground motions are simulated using kinematic model for the NTF scenario, which is the most important fault scenario for Tabriz City. A finite fault model with non-uniform slip distribution on the fault plane (asperity) is assumed. Different rupture scenarios of NTF are examined to find the source parameters for the worst rupture scenarios. Then, the velocity ground motions are simulated at 300 points, which cover whole Tabriz region by a 1 km × 1 km grid size. The simulated ground motions in near-fault area consistency show a forward directivity pulse that its period and peak value show significant variation with respect to the site to source distance and rupture nucleation point. Finally, the PGV and PSV microzonation maps are provided for Tabriz City.

2. GEOLOGIC SETTING OF NORTH TABRIZ FAULT

The NTF is the most prominent tectonic structure in the immediate vicinity of Tabriz City. It can be followed almost continuously at the foot of the northern mountains near Tabriz for about 100 km, from Mishu mountain in the west to Bosatabad in the east. The fault trace is approximately N115° E and its dip is vertical (Fig. 2.1). Hessami et al. (2003) performed geomorphic and trenching investigations, which allowed them to recognize evidence for repeated faulting events since the Late Pleistocene. From the trenches they found evidence for at least four events during the past 3.6 ka, the most recent one being the 1780 earthquake. On the basis of different approaches, horizontal slip per event and slip rates are found in the ranges of 4± 0.5 m and 3.1-6.4 mm/yr, respectively. They also attempted an estimate of the average recurrence intervals which appears to be in the range of 350-1430 years, with a mean recurrence interval of 821±176 years.

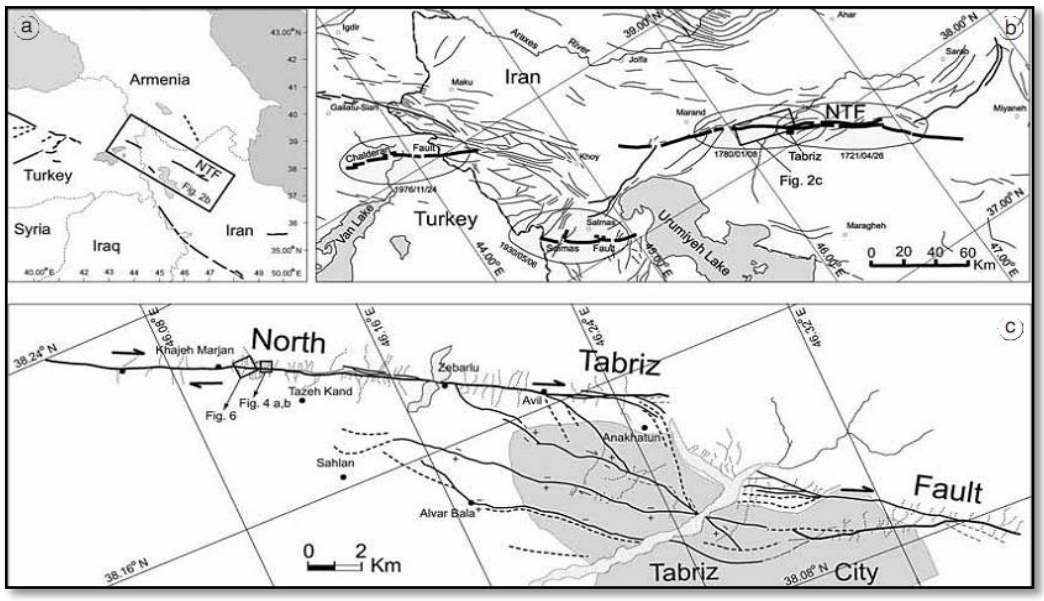

Figure 2.1. a) Small-scale regional map of active faults in NW Iran-Eastern Turkey (after Jackson and McKenzie, 1984). Rectangle encloses Fig 2.1.b) Simplified map of the NTF and location of historical earthquake, modified after Berberian (1997). Rectangle encloses Fig. 2.1c) NW section of the North Tabriz Fault (after Karakhanian *et al.* 2001, Hessami et al. 2003).

3. KINEMATIC METHOD

Ground motion from an earthquake can be simulated if a slip distribution across a fault surface (i.e. source effects) and a Green's function, which represents the impulse response of propagation medium (i.e. propagation path effects), are known. There are two ways to characterize a fault motion at an earthquake source, namely kinematic and dynamic source models. The kinematic source models give arbitrarily the slip space-time functions on the fault plane without physical considerations regarding stress conditions. In spite of the inadequacy in the handling of the physical condition in the source, the kinematic model yields numerous important results in interpreting ground motions from earthquakes and in estimating slip distributions and rupture propagating over the fault planes. Haskell (1964) made the pioneer work on kinematic model to express the source effect defining fault length, fault width, final slip, rise time, and rupture velocity. This method has been widely employed in determining source characteristics of large earthquakes (Ghayamghamain and Hisada 2007b).

Starting from representation theorem (Aki & Richards, 1980), it can be shown that in homogenous, isotropic, and infinite medium, the displacement $\vec{u}_i(\vec{x},t)$ of P and S waves at point $(\vec{x},t)$ due to a displacement discontinuity $\vec{u}\,(\vec{\xi},\tau)$ at point $(\vec{\xi},\tau)$ across an internal surface $\sum$ can be given by:

$$\overrightarrow{u_\iota}(\vec{x},t) = \frac{R_c(\phi,\delta)}{4\pi\rho c^3 r}\cdot\mu\iint_{\Sigma}\Delta\dot{U}_J\left(\vec{\xi},t-\frac{r}{c}\right)d\Sigma \tag{3.1}$$

Where μ is the rigidity, r is the distance between the fault plane Σ and point of observation, R_c (subscript c indicates the wave type: P, SV or SH) is the radiation pattern coefficient along the strike ϕ and dip δ of the fault. The function Δu is a scalar, called the "source function" or the "slip function" in case of a shear fault. For a fault of length L and width W, the displacement waveform can be written in a simple form given by:

$$\overrightarrow{u_\iota}(\vec{x},t) = \int_0^L\int_0^W \Delta\dot{u}\,(\xi,\eta) * \vec{G}(\vec{x},\xi,\eta,t)d\xi d\eta \tag{3.2}$$

Where G is the Green's function, and $*$ represent convolution. To simulate ground motion due to an extended fault, the fault surface is divided into small sub-faults. Assuming that the fault plane is divided into l elements along the strike of the fault and m elements along its down-dip direction, the above integral can be rewritten in the following form:

$$\overrightarrow{u_\iota}(\vec{x},t) = \sum_{i=1}^{l}\sum_{j=1}^{m}\int_{L_i}^{L_i+\Delta L_i}\int_{W_i}^{W_i+\Delta W_i}\Delta\dot{U}\left(\xi_i,\eta_j,t-\tau_{ij}\right) * \vec{G}\left(\vec{x},\xi_i,\eta_j,t\right)d\xi d\eta \tag{3.3}$$

Where τ_{ij} is the time taken by the rupture front to propagate from hypocenter to the i, j the sub-fault. The rise time of the dislocation function is small for the smaller event and is also scaled by the similarity condition of earthquakes as:

$$\frac{\tau}{\tau_e} = \left(\frac{M}{M_e}\right)^{1/3} \tag{3.4}$$

(Kanamori and Anderson, 1975; Hardly and Helmberger, 1980; Irikura, 1983), where the parameters with a subscript e correspond to the small earthquake and without, to the large earthquake. M is the seismic moment of an event. The above ratio is a constant and is approximated by an integer n. Thus, $\vec{u}\,(\vec{x},t)$ can be expressed as:

$$\overrightarrow{u_i}(\vec{x},t)=\sum_{k=1}^{n}\sum_{j=1}^{m}\sum_{i=1}^{l}\int_{L_i}^{L_i+\Delta L_i}\int_{W_i}^{W_i+\Delta W_i}\Delta\dot{U}\left(\xi_i,\eta_j,t-\tau_{ij}-(k-1)\right)*\vec{G}\left(\vec{x},\xi_i,\eta_j,t\right)d\xi d\eta \quad (3.5)$$

Where *k* is a random number, which prevents an artificial periodicity in simulated motion (Joyner and Boore, 1988). Equation (3.5) is the base of simulation studies that have been done to date. The parameter *n* is the number of sub-sources per sub-fault. The simulated motion of the large event is then the summation of contributions from *l* fault element along strike, *m* fault elements down-dip and *n* source functions lagged in time on each fault element. For Green's function, the one developed by Aki and Richards (1980) for homogeneous, isotropic and unbounded medium is used here.

4. SOURCE PARAMETERS AND SIMULATION POINTS

For our simulation, we chose 60 km of the Tabriz fault, which is segment close to the Tabriz City as shown in Fig. 4.1. The areas on the fault rupture surface that have large slip relative to the average slip are defined as "asperities". The asperities have a large influence on ground motion estimation, especially in near-fault area (Ghayamghamian and Hisada 2007, Ghayamghamian 2003).The area and slip of the asperity are estimated using the relations developed by Somerville et al (1999) based on the analysis result from 15 crustal earthquakes. Then, a single asperity with area and slip of 225 km^2 and 335 cm, respectively, were assumed (Fig. 4.2). It should be mentioned that the number of asperity could be assumed larger than one. However, since we are interested only on the peak ground velocity, only the largest asperity is modeled in the analysis. Different configurations of asperity and rupture nucleation point are examined to find the worst rupture scenario of NTF. To this end, the PGV at some key sites in Tabriz were simulated and compared for different source configurations. The final fault model is shown in Fig. 4.2 and its rupture parameters are summarized in Table 4.1. Then, the Tabriz region was divided into 300 grids with a grid size of 1 km × 1 km to simulate velocity waveforms, and to compute PGV microzonation maps of Tabriz. Fig. 4.1 shows the simulation points assigned for Tabriz region.

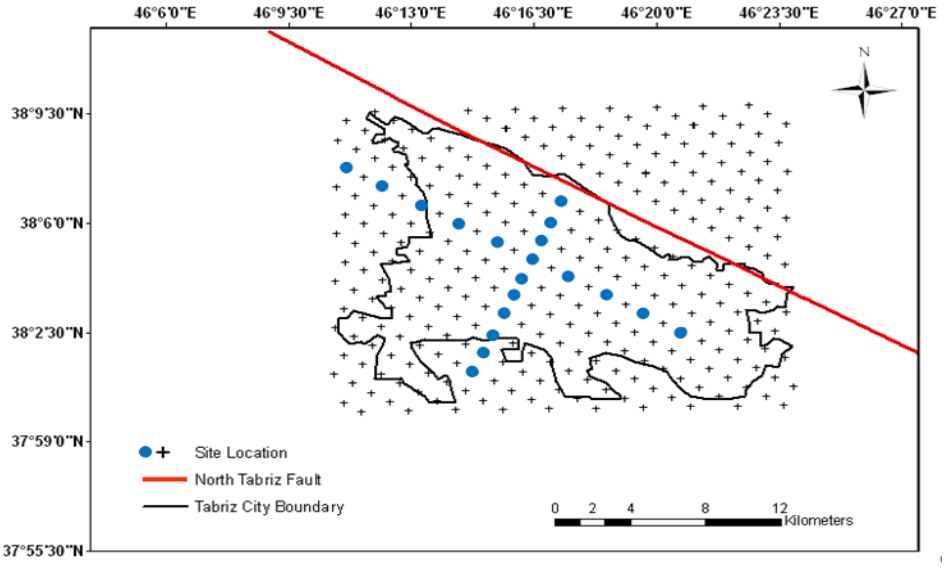

Figure 4.1. The location of NTF with boundary of Tabriz City in the background. The circle and plus signs show the location of the sites where the ground motions are simulated.

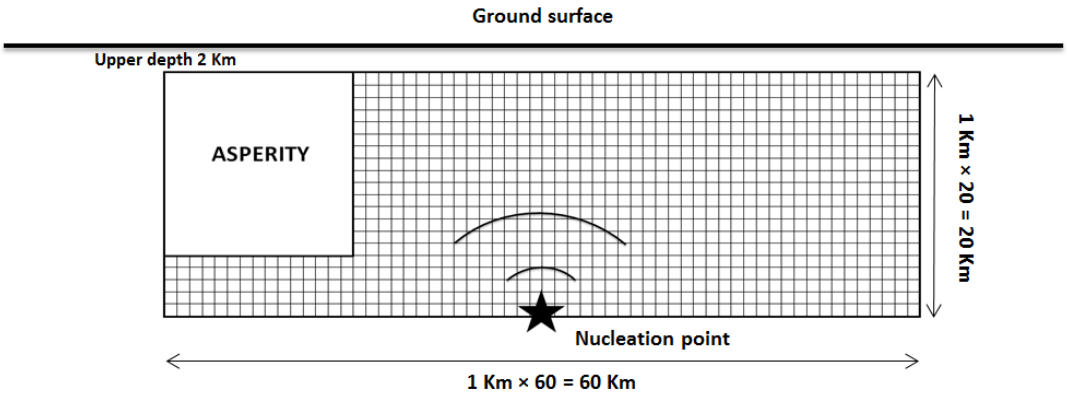

Figure 4.2. Schematic figures showing location of asperity, nucleation point and rupture directions on the fault plan.

Table 4.1. Source parameters for NTF scenario.

source parameters	Value
Mw	7.3
Fault length	60 km
Fault width	20 km
Dip	90°
Strike	115°
Rake	0°
Max. slip of asperity	335 cm
P-wave velocity	6 km/s
S-wave velocity	3 km/s
Raise time	1s
rupture velocity	2.5 km/s

5. LONG-PERIOD GROUND MTION SIMULATION IN TABRIZ

The long-period ground motion is simulated at 300 points covering whole Tabriz region. To show the variation of simulated motions, the velocity waveforms at the 20 sites, which are located along two perpendicular and parallel lines to the fault strike (see bold circles in Fig. 4.2), are shown in Fig. 5.1. From this figure, a clear rupture directivity pulse with the peak values of 40 to 65 cm can be seen in the NS component, which is almost oriented to the fault normal (FN) direction.

The rupture directivity pulse characteristics vary with respect to the sites distance from the source and its azimuth. The PGV at the sites in perpendicular direction to the fault strike decreases with distance from the fault. Furthermore, the response spectra of the simulated velocity ground motions were also calculated for the 20 sites as shown in Fig. 5.2. The velocity response spectra also show with maximum values of 55 to 120 cm/sec at period range of 0.7 to 1 sec. The velocity response spectra characteristics also vary with respect to the sites location. The PSV and the period of maximum values of velocity response spectra at the sites in perpendicular direction to the fault strike with distance from the fault, decreases and increases, respectively. From the estimated peak values of velocity time histories at the sites, the PGV microzonation map of Tabriz City is also developed as shown in Fig. 5.3. The PGV is found to be in the range of 100 to 255 cm/sec and with maximum value of 255 cm/sec in the north of Tabriz City. In the same way, the microzonation map for peak spectral velocity (PSV) is also developed as shown in Fig. 5.4. The PSV in found to be in the range of 200 to 330 cm/sec with maximum value of 330, also in the north of Tabriz City.

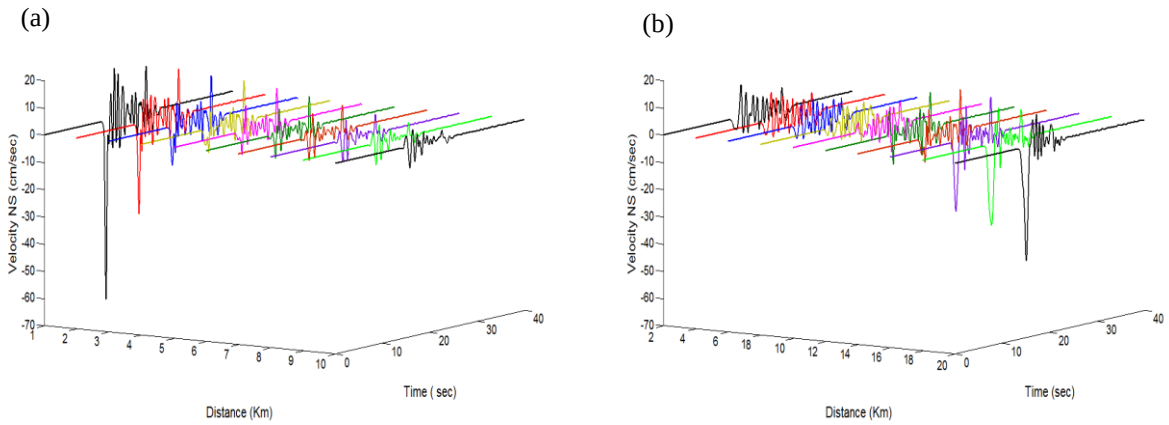

Figure 5.1. Simulated velocity wave forms for NS components at 20 sites which are located along a line (a) perpendicular to the fault strike in 1 km distance and (b) parallel to the fault strike in 2 km distance.

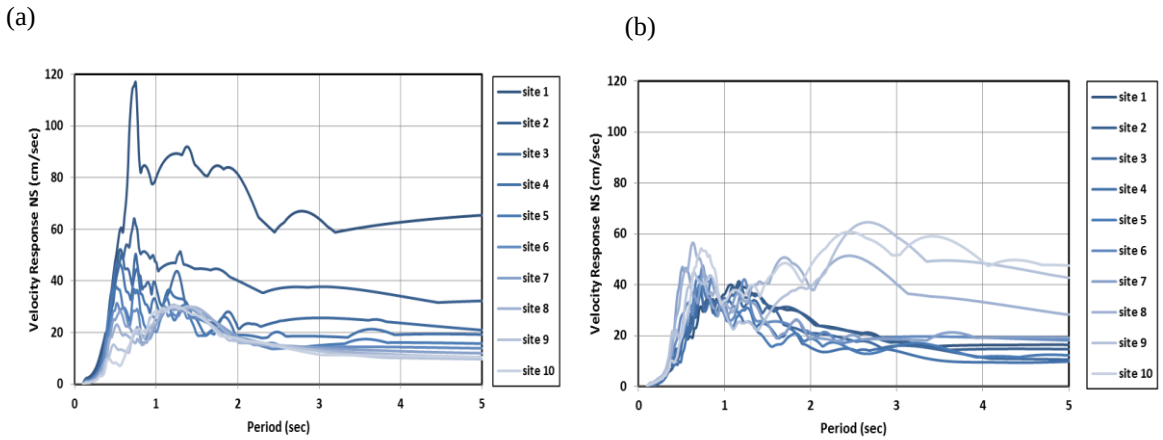

Figure 5.2. The velocity response spectra of simulated motions for NS components at 20 sites, which are located along a line (a) perpendicular to the fault strike in 1 km distance and (b) parallel to the fault strike in 2 km distance.

6. CONCLUSION

In this paper, the long-period velocity waveforms were simulated using kinematic method for NTF scenario. The worst rupture scenario was defined for different configurations of source parameters such as asperity and nucleation point locations on the fault. The velocity time histories were simulated at 300 sites covering whole Tabriz region. The rupture directivity pulse characteristics vary with respect to the sites distance from the source and its azimuth. The simulated motions consistently show a near-fault directivity pulse with maximum PGV value in the ranges of 50 to 255 cm/sec. Furthermore, the response spectra of the simulated velocity ground motions were also calculated and their peak values are found to be in the range of 150 to 330 cm/sec. The maximum peak ground velocity and peak spectral value are shown to be in the north of Tabriz City. Finally, the calculated peak values for velocity waveforms and spectral velocities were used to develop the PGV and PSV micozonation map, respectively.

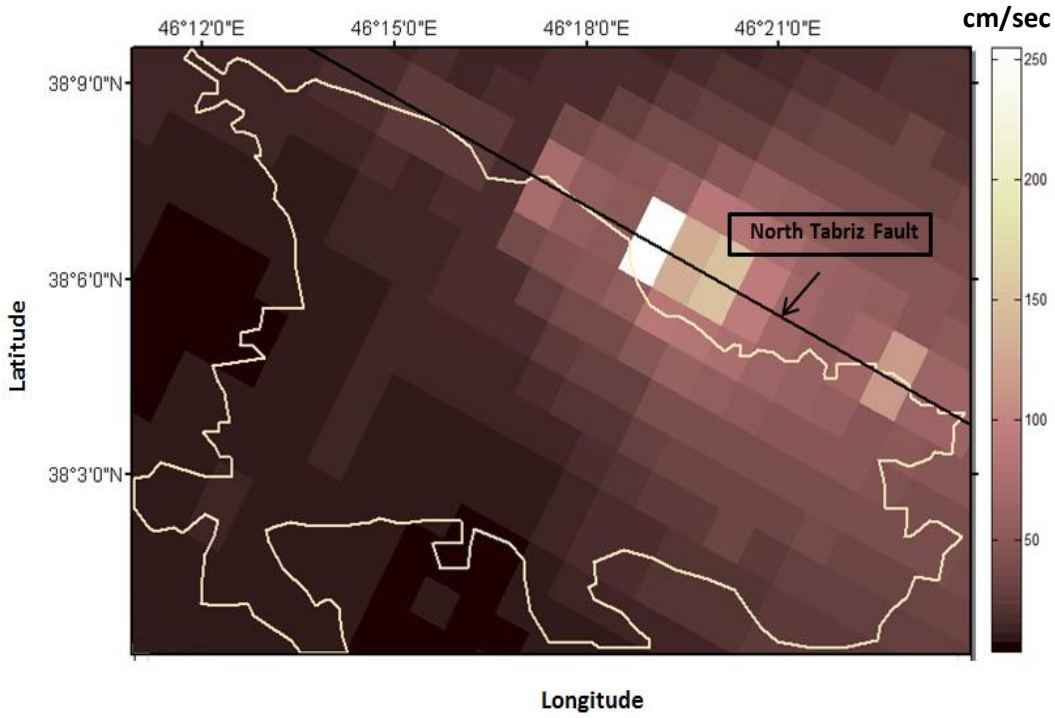

Figure 5.3. PGV microzonation map of Tabriz City based on estimated PGV at 300 sites where the velocity ground motions are simulated.

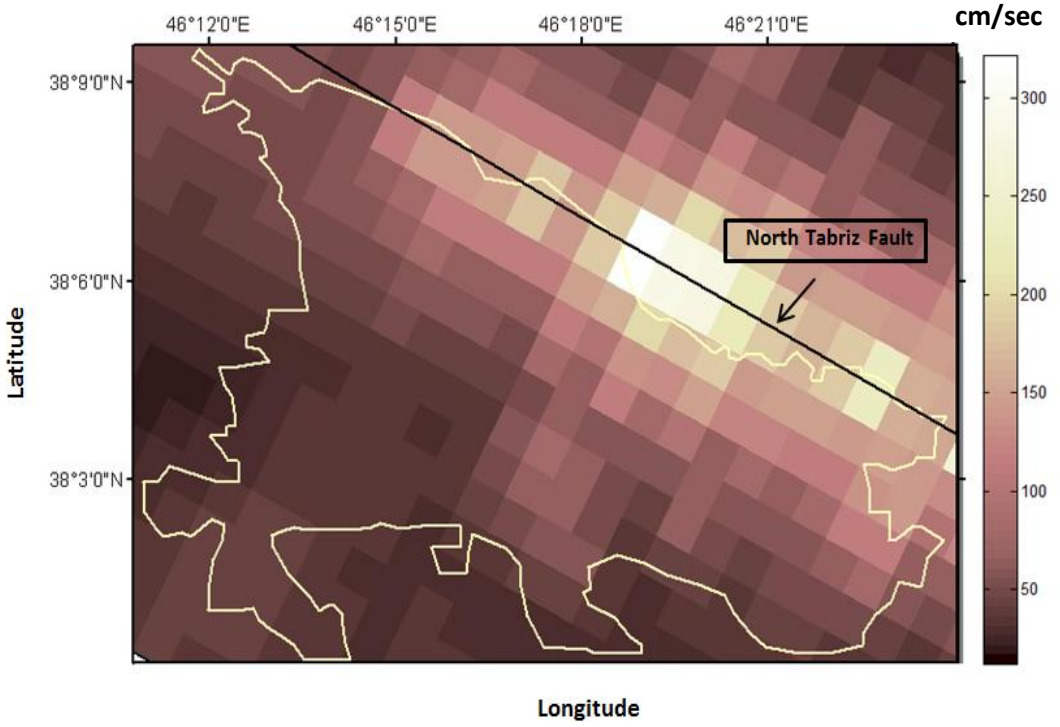

Figure 5.4. Peak spectral velocity (PSV) microzonation map of Tabriz City based on spectral peak values of computed response spectra at 300 sites where the velocity ground motions are simulated.

REFERENCES

Aagaard, B. T., Hall, J. F., and Heaton, T. H., 2000.Sensitivity study of near-source groundmotion, Proceedings of the *12th World Conference on Earthquake Engineering*, New Zealand Society for Earthquake Engineering, Upper Hutt, New Zealand.

Aki K., Richards P.G., 1980. Quantitative Seismology: Theory and Methods, W.H. Freeman and Co. New York.

Alavi, B. and Krawinkler, H., 2004.Behavior of moment-resisting frame structures subjected to nearfault ground motions.*Earthquake Engineering and Structural Dynamics*.**33:687–706** (DOI: 10.1002/eqe.369).

Alavi, P., Krawinkler, H., 2001. Effects of near-fault ground motion on building structures, CUREE-Kajima Joint Research Program Report, Richmond, California.

Ambraseys, N. N., Melville, C. P., 1982. A history of Persian earthquakes. Cambridge University press, New York: 219.

Baker, J. W., Cornell C. A., 2005. A vector-valued ground motion intensity measure consisting of spectral acceleration and epsilon. *Earthquake Engineering and Structural Dynamics***; 34:1193–1217**.

Berberian, M., 1983. The southern Caspian: A comparison depression floored by a trapped, modified oceanic crust. Can J Earth Sci**20:163-183**

Bertero, V. V., Mahin, S. A., Herrera, R. A., 1978. A Seismic Design Implication of Near fault San Fernando Earthquake Records. *Earthquake Engineering and Structural Dynamics*.**6: 31-34**.

Fu, Q., 2005. Modeling and Prediction of Fault-Normal Near-Field Ground Motions and Structural Response, Ph.D. Dissertation, Department of Civil and Environmental Engineering, Stanford University, CA.

Ghayamghamian M.R., 2007a. Directional damage due to near-fault and site effects in the M6.4 Changureh-Avaj earthquake of 22 June 2002.*Journal of Seismology*.DOI 10.1007/s10950-006-9026-y.

Ghayamghamian, M. R., Hisada, 2007b. Near-fault strong motion complexity of the 2003 Bam earthquake (Iran) and low-frequency ground motion simulation. *Geophysical Journal International*, Vol**170**, No. **2**, PP. 679-686(8).

Ghayamghamian M.R., 2003. Near-field ground motion simulation for heterogeneous faulting, *4th Inter. Conf. on Earth. Eng. &Seis*., Tehran, Iran.

Hall, J.F., Heaton, T.H., Halling, M.W. and Wald, D.J., 1995. Near-source ground motion and its effects on flexible buildings. Earthquake Spectra 11:4, 569-605.

Hessami, K. Pantosti, D. Tabassi, H. Shabanian, E. Abbassi, M. Feghhi, K. Solaymani, S., 2003. Paleoearthquakes and slip rates of the North-Tabriz Fault, NW Iran.Preliminary Results. *Annals Of Geophysics*, Vol**. 46**, No. **5**.

Irikura, K., 1983. Semi-empirical estimation of strong ground motions during large earthquakes.*Bulletin, Disaster Prevention Research Institute*. Kyoto University, Kyoto, Japan, Vol33:63-**104**.

Iwan, W.D., Huang, C. and Guyader, A.C., 2000. Important features of the response of inelastic structures to near-field ground motion. *12th World Conference on Earthquake Engineering [Proceedings on CD]*.Paper No. 1740, New Zealand Society for Earthquake Engineering, New Zealand.

Joyner, W. B., and D. M. Boore (1988). Measurement characterization, and prediction of strong ground motion, Earthquake Engineering and Soil Dynamics II – Recent Advances in Ground Motion Evaluation, ASCE, 43-102.

MacRae, G. A., Morrow, D. V., Roeder, C. W., 2001. Near-fault ground motion effects on simple structures, J. Struct. Eng. ASCE **127: 996–1004**.

Masson, F., Van Gorp, S., Chéry, J., Djamour, Y., Tatar, M., Tavakoli, F., Nankali, H., Vernant, P., 2006, Extension in NW Iran Driven by the Motion of the South Caspian Basin, *Earth Planet. Sci. Lett.*, **252: 180-188**.

Mavroeidis, G. P., and Papageorgiou, A. S., 2003. A mathematical expression of near-fault ground motions, Bull. Seismol.Soc. Am. 93 _3_, 1099–1131.

Singh, J. P., 1985. Earthquake ground motions: Implications for designing structures and reconciling structural damage, Earthquake Spectra 1, 239–270.

SomerVille P. , Irikura K. ,Graves R. , Sawada S. , Wald D. , Abrahamson N. , Iwasaki Y. , Smith N. , Kowada A., 1999. Characterizing Crustal Earthquake Slip Models for the Prediction of Strong Ground Motion. *Seismological Research Letters*.Vol**70.** No **1**.

Somerville, P. G., 2003. Magnitude scaling of the near fault rupture directivity pulse.Phys. Earth Planet.Int. 137, no. 1, 12.Seism. Res. Lett. 68, no. 1, 199-222.

Somerville, P.G., Smith, N.F., Graves, R.W., Abrahamson, N.A., 1997.Modification of Empirical Strong Ground Motion Attenuation Relations to Include the Amplitude and Duration Effects of Rupture Directivity. *Seismological Research Letters.***68:199-222**.

Tothong, P., Cornell, C. A., 2006a. Probabilistic Seismic Demand Analysis Using Advanced Ground Motion Intensity Measures, Attenuation Relationships, and Near-Fault Effects, Pacific Earthquake Engineering Research Center, PEER Report 2006/11, University of California, Berkeley, 2007, 205 pp.

Wald, D. J., Heaton, T. H., 1998. Forward and inverse modeling of near-source ground motions for use in engineering response analysis, Paper T162-1, Proceedings of the American Society of Civil Engineering, San Francisco.